MESOSCALE WAKE CLOUDS IN SKYLAB PICTURES

FINAL REPORT

TO

NATIONAL AERONAUTICS AND SPACE ADMINISTRATION

LYNDON B. JOHNSON SPACE CENTER

UNDER

CONTRACT NO. NAS 9-14042

PREPARED BY

T. THEODORE FUJITA AND JAIME J. TECSON

THE UNIVERSITY OF CHICAGO

AUGUST 1, 1974

CONTENTS

Mesoscale Wake Clouds in Skylab Pictures

by

T. Theodore Fujita and Jaime J. Tecson

Department of Geophysical Sciences
The University of Chicago
Chicago, Illinois 60637

Abstract

Since Mariner 9 observation of wave clouds on Mars, the recognition of cloud patterns in the wake of orographic obstacles has become an important tool in estimating atmospheric motions. Island-wake clouds have long been identified as so-called Kármán vortices. Skylab pictures revealed, unexpectedly, the existence of ship-wake-type wave clouds in contrast to vortex streets.

Skylab pictures were examined in detail in an attempt to characterize the pattern of waves as well as the transition between waves and vortices. Presented in this paper are examples of mesoscale cloud patterns analyzed photogrammetrically and meteorologically.

1. INTRODUCTION

The manned Skylab flight, with its capability of taking photographs of the terrestrial objects in any direction within its track at its vantage distance in space, and with the ability of the mission crew, of course, to make instantaneous decisions on recording unique events or occurrences it deems worthwhile, has provided unusually fine-quality and remarkable pictures of mesoscale phenomena worthy of investigation.

Mesoscale circulations characterized by wake waves and by vortices are produced in certain limited areas of the globe under favorable conditions. Though these circulations do not affect large areas, yet these phenomena should be significant enough in the synoptic conditions of the local areas and possibly in the pollution of some other areas.

Remarkably enough, Mariner 9 photographs of the atmosphere of Mars, showing impressive wave-cloud patterns caused by its craters have been identified by Briggs and Leovy (1974). Interest in the mesoscale phenomena has been renewed. Chopra and Hubert (1964, 1965) have found a quantitative analogue to the island patterns in the vortex streets formed behind a solid cylinder comparable in size to the islands. They have found apparent resemblance between the meteorological mesoscale eddies and the classical vortex street pattern. Formations of cumulus streets and observance of cloud-free paths under winter monsoon situations in certain areas have been investigated by Tsuchiya and Fujita (1966).

It is encouraging to note that Skylab orbital altitude assures high-quality resolution photographs detailing the fine structures of the mesoscale-size phenomena observed within its path. Investigations therefrom could yield to more meaningful evaluations.

2. WAKE WAVES OF BOUVET ISLAND IN THE SOUTH ATLANTIC

A spectacular sequence of three pictures, SL 4-3631, -3632 and -3633, shows a pattern of wake waves which are expected to be found behind a moving ship.

The picture catalog suggests that the source of the wake waves is Diego Alvarez (Gough) Island. Meanwhile, the HDC CX 47 #78, 79, 80 were exposed at 1423 GMT on Day 349 or December 15, 1973 to show "Island Wake in Stratus; 4°W, 48°S; wake toward the East; 150 mile long with 20-30 crests and valleys under high sun angle".

A composite of hand-rectified cloud pattern revealed, however, that the island is located to the south of the Skylab orbit 3104 with the 80 W crossing time of 1405 GMT.

An attempt was made to semi-rectify the picture SL 4-3633, the last picture of the sequence. The result is presented in Fig. 1. Bouvet Island is located at 54°26'S and 3°24'E. The elevation of the island is 935 m (3068 ft).

The center of the wake as indicated by a wavy dotted red line suggests a sinusoidal fluctuation of the southwesterly flow against the island. The vertex angle of the wake boundaries is computed to be 38 degrees which is very close to the case of a moving ship.

A strange thing is the outward extension of the lateral waves which are commonly seen only inside the vertex angle of a ship wake. It may be possible, though, that configurations of this form could arise. Stoker (1957) has mentioned that the disturbance or surface waves created by a moving ship is not exactly zero outside the region of disturbance, but rather it is small and of a different order from a disturbance inside that region. In view of this, while water waves cannot normally be detected outside the region of disturbance, the vertical velocity in the atmospheric case is small but non-zero in said region. In a saturated layer, therefore, even such a small vertical velocity may be of such

magnitude to produce clouds and hence reveal the existence of such wave clouds extending beyond the region of disturbance. It is hard to understand, though, how the wave energy is transported outward into a large vertex angle of about 90 degrees.

The half amplitude of the waves is estimated to be the island elevation of about 1 km. The wave length varies between 10 and 15 km which is one order of magnitude larger than the amplitude. The depth of the atmosphere below the wave would be only about 1 km suggesting that the trough just behind the island might be practically on the ground.

The evidence seen in the picture reveals that the waves, by no means, correspond to the deep-water ocean waves. The kinetic energy of the waves are likely to be lost very quickly.

It would be of extreme value if we are able to investigate the mechanism of wave propagation within and just outside of the vertex angle behind such an island.

3. COMPARISON WITH SHIP WAKES

Kelvin's (1887) theory of wave patterns created by a moving ship indicates that the V-shaped pattern behind a moving object is similar regardless of the object size as long as the motion is steady along a straight line course. When an object, ranging from a duck to a battleship moves, a moving pressure point is created, resulting in a stationary phase.

The vertical displacement of the water surface at a given point is the integrated effect of the point impulse which moves with an object. When the water is infinite in depth, the points influenced by an object at a specific time moves at the rate of one-half of the speed of the object. The instantaneous positions of influence point are located on

a circle through the ship's position at the specific time. The diameter of the circle coincides with the instantaneous velocity of the ship. The outer boundaries of the V-shaped wake behind the ship are the envelopes of successive circles with increasing diameter in proportion to the distance from the moving ship or obstacle.

The vertex angle is, thus, expressed by

$$2 \text{ arc sin } \frac{1}{3} = 38°56'$$

which is a constant independent of the object size and speed, so long as the object's velocity is constant.

Waves caused by a moving pressure point, like that of a moving ship, are confined to a region of disturbance behind the ship. In particular, there are two distinct set of waves apparent in conformity with the fact that each point in the disturbed region corresponds to two influence points: one set which is arranged roughly at right angles to the ship's course, and another set which seems to emanate from the ship's bow. These two systems of waves are called the transverse and diverging waves, respectively. The first type, the TRANSVERSE WAVES, connect, more or less, the left and right edges of the V-shaped wake.

The second type, called the DIVERGING WAVES, are characterized by the maximum amplitude near the wake boundaries. These waves diverge outward with their amplitudes decreasing practically to zero at the wake boundary.

Shown in Figs. 2 and 3 are the wake waves seen behind moving ships in a lake. Figure 2 was taken over Lake Michigan while Fig. 3 was shot over a lake in northern Indiana, both on July 13, 1974. One of the major differences in the pattern of the wake waves is the existence of the transverse waves in Fig. 2.

Havelock's (1950) solution of finite depth waves indicates that the transverse waves disappear when

$$\frac{c^2}{gh} > 1$$

where c is the ship's speed, g, the gravity, and h, the depth. If we assume the depth of Lake Michigan (Fig. 2) to be 30 m and c = 5 m/sec, we have

$$\frac{c^2}{gh} = \frac{25}{9.8 \times 30} \cong 0.1$$

This would suggest the existence of the transverse waves.

The Indiana lake was very shallow, while the speed boat was running very fast. If we use the figures, c = 10 m/sec and h = 5 m, we have

$$\frac{c^2}{gh} = \frac{100}{9.8 \times 5} \cong 2$$

which is considerably larger than 1 when the transverse waves are expected to disappear. As seen in Fig. 3 the wake is characterized by diverging waves only.

Above examples and discussion on ship wakes suggest that the wave patterns are characterized by:

A. Diverging and Transverse Waves exist when a ship moves slowly on a deep water surface (slow-moving air with deep layer below the inversion surface).

B. Diverging Waves exist only when a ship moves fast on a shallow water surface (fast-moving air with shallow layer below the inversion surface).

The law of similarity between ship wakes and island wakes has not been established. It is because the dimensions of island will have to be taken into consideration that the wakes of a television tower and a volcanic island are known to be entirely different.

4. WAKE WAVES AND VORTEX STREETS FROM ALEUTIAN ISLANDS

On January 14, 1974, the Aleutian Islands were under the influence of moderate

easterly winds ranging between 10 to 15m/sec (20 to 30 kt). The upwind side of the island was covered with stratus with their tops at about 1000 m MSL.

Near the end of the Orbit 3529, two successive pictures of Aleutian Islands were taken at 0143 GMT, January 14, 1974. The picture subpoint and the photographic coverage are indicated in Fig. 4, showing the surface conditions at 0000 GMT less than two hours before the pictures. The surface map reveals that the flow near the southern tip of the photo-area is uniform: 12 m/sec from the 120-degree direction.

Under such a uniform flow, what nature created were both waves and eddies. Figure 5 is a gridded version of SL 4-4111 and 4112. Two pictures were combined into one image prior to the gridding at 1-degree interval of longitudes and latitudes. The picture covers a 700-km island chain extending from Amukta to Unimak Islands.

Van Kármán vortices are seen predominantly in the wakes of large orographic features such as Mt. Vsevidof, Okmok Crater, Makushin Volcano, Pogromni Volcano, and Isanotski Peaks. P is the largest eddy produced in this island chain. Meanwhile, the wake waves, mostly diverging waves in nature, are found behind small islands. Since the characteristics of the flow are uniform, the major factor in producing waves and vortices is suspected as being the dimensions of the obstacles.

Figure 6 was constructed by rectifying SL 4-4111 into 1:1,000,000 scale. It should be noted that small peaks are generating a long wake with diverging waves. From this picture along with SL 4-4112, a table of wake characteristics is produced (Table 1).

The width of the obstacles in the table is defined as being the cross-sectional dimension of the 300-m elevation.

The table reveals that the critical dimension of the obstacle between the wave and eddy formation is 5 km. If an obstacle is 5 km wide or smaller, diverging waves

Table 1. Wake Characteristics of Aleutian Islands January 14, 1974

Obstacles	Longitude	Height (m)	Width (km)	Wake Type
Amukta Volcano	171°15'	1056	4	Diverging waves
Chagulak Island	171°09'	1143	2	Diverging waves
Yunaska Island	170°48'	951	5	Diverging waves
Yunaska Island	170°39'	600	4	Diverging waves
Herbert Island	170°07'	1288	5	Waves + eddies
Carlisle Island	170°04'	1610	5	Waves + eddies
Mt. Cleveland	169°57'	1730	5	Eddies
Chuginadak Island	169°46'	1170	8	Waves + eddies
Uliaga Island	169°46'	888	2	Diverging waves
Kagamil Island	169°43'	893	2	Diverging waves
Mt. Vsevidof	168°31' & 42'	1984 & 2109	24	Vortex street
A Small Peak	168°18'	610	5	Diverging waves
Tulik Volcano	168°08'	1253	22	Vortex street
Makushin Volcano	166°56'	2036	32	Vortex street
Akutan Island	166°00'	1303	12	Vortex street
Pogromni Volcano	164°42'	2002	19	Vortex street

form in the island wake. The height of the obstacle does not influence the wake characteristics as long as the obstacle extends beyond the top of the stable layers.

Laboratory estimates on vortex streets have shown that the Reynolds number (Re) for the lower limit for stable vortex formation is 35. The kinematic eddy viscosity (ν) corresponding to the critical diameter of the orographic obstacle can be computed from

$$\nu = \frac{DU}{Re} = 2.4 \times 10^7 \text{ cm}^2/\text{sec}$$

where D = 5000 m, and the geostrophic wind (U) = 17 m/sec. This value is in conformity with that estimated by Chopra and Hubert (1964).

5. KÁRMÁN VORTEX STREETS FROM KURIL ISLANDS

Vortex streets under a very weak flow condition developed in the wake of Kuril Island on June 4, 1973 of which SL 2-432 was photographed at 0000 GMT (Orbit 293).

The picture was rectified into Fig. 7 with overlays showing island topography in blue and vortex patterns in red. Of interest is the change in the flow direction within a short distance along the island chain.

The weather report via Tokyo indicates that Urup Island at 0000 GMT was 1° C with 1 m/sec wind from the 320°. The air was practically calm there. The large-scale flow as estimated from the wake vortex pattern is anticyclonic with a southerly flow between Iturup and Urup Islands. A small cyclonic eddy is seen off the north of Iturup. The northern wake of Iturup is clear suggesting a southerly flow there.

A cyclonic eddy to the northeast of Urup suggests the existence of a southwesterly flow along the southeast coast of the island. Off the southwest tip of Simushir, a weak northwesterly is in existence. A similar flow prevails across the islands of Ketoy, Rasshua, and Matua.

Climatologically speaking, the sea-surface temperature in June around Matua Island is known to be the coldest in the Kuril chain. Practically every day, low stratus and fog cover the area suggesting the existence of a semi-permanent inversion layer. The stratification is, therefore, favorable for the development of vortex streets behind the island.

It is rare, however, to observe a significant change in the flow patterns as shown in the SL 2-432 picture.

6. BLOCKING OF EVAPORATION CUMULI BY ALEUTIAN ISLANDS

It has been well known that cumulus streets form when dry cold air of polar-continental origin passes over an ocean. Transported from the ocean surface to the atmosphere are heat and moisture. When the rate of transportation is very large, the initial formation of cumuli takes place only few miles off shore.

Skylab pictures show numerous examples over the Great Lakes, off the Japan Sea coast of Siberia, off the Atlantic coast of the United States and other areas.

One of the most striking pictures of such evaporation cumuli is SL 4-4210 (Fig. 8) taken at 0106 GMT on January 17, 1974 during the Orbit 3572. The picture was taken looking north toward Alaska Peninsula.

As shown in Fig. 9, the center of a well-developed cyclone with the central pressure of 965 mb was located in the Gulf of Alaska. The central pressure is so low that it is comparable to that of an intense hurricane.

The air temperature in Yukon is 40° C below zero. A strong surge of cold air is seen in the northwest sector of the cyclone. The wind speed along the Alaskan coast is about 10 m/sec from the north.

A gridded picture of SL 4-4210 reveals a very narrow cloud-free area along the coast of Kuckokwin Bay, Etolin Strait, and Hazen Bay. The cloud-free path of the cold-air outflow is only several miles.

After the formation of evaporation cumuli, cloud streets develop in the direction parallel to the flow. Numerous streets are seen to extend from the formation points toward the Alaskan Peninsula.

The blocking of these cumulus streets by mountains in the Peninsula is of extreme interest. A similar phenomenon is frequently seen over Japan under the winter monsoon but not in the Atlantic off the east coast where no blocking mountains exist.

Both waves and vortices in the wake regions are insignificant or non-existent. A number of high peaks in the Peninsula simply block the cumulus streets over the Bering Sea. Those cloud streets which are seen to the south of the Peninsula originate in the low gaps where leakage of moisture from Bering Sea takes place.

A most significant cloud-free dark spot is seen to the south of Mt. Veniaminof, a 2560-m peak. An insignificant eddy street extends downwind from the peak region. Another dark spot is found in the wake of Pavlof Volcano of 2718-m elevation. Coast lines are visible within these dark spots which are cloud free, being dominated by strong downslope winds.

What are the reasons for not seeing waves and vortices within the obstacle wake in this case? One of the reasons appears to be the temperature lapse rate of the air just above the sea surface. If the lapse rate is adiabatic or very close to it, the vertical mixing is stimulated by the eddy transport. Such a mixing process will effectively damp out both waves and eddies, thus restricting their transport downwind inside the wake regions.

7. THERMAL AND MECHANICAL EFFECTS OF SOUTH PACIFIC ISLANDS

An interesting sequence of five pictures was taken from near New Zealand looking toward the south or southeast in the Skylab Orbit 3211. These pictures are SL 4-3701 through 3705.

Picture subpoints and the direction of the principal lines are shown in Fig. 10, a surface map of New Zealand area at 0000 GMT December 23, 1973. It is seen that the first two pictures were taken looking toward the Auckland Island and Campbell Island areas. The next two pictures, 3703 and 3704, show beautiful wake waves extending downwind from Campbell Island. The last picture of the sequence shows cloud formations near Chatham Island generating several cumulus streets acting as a heated island.

Figure 11 with a blue overlay shows an existence of cumulus streets originating over Chatham and Pitt Islands. The largest street extending from the northern part of Chatham originates on the coast line. Since a cloud line often originates over a flat plane downwind from a pointed cape or peninsula, the point of origin of the cloud line could be within the pointed peninsula.

Another cloud line originates within a peninsula extending into Te Whanga Lagoon, the largest one on the island. There are 5 cloud lines starting from high spots of southern Chatham. Each cloud line or plume near the source extend toward the 250 to 260 degrees. As the plume leaves the source its direction changes into 230 degrees, suggesting that the plume direction changed into that of the gradient wind over the island.

Cloud lines from Pitt Island are very important in terms of their appearance. With the exception of the central plume originating from the 296-m peak, the other three take a shape of the diverging waves. The microscale pattern of the plumes imply that they consist of small cumulus cells. However, the island-scale pattern of the plumes

shows a configuration of three diverging waves. Further examination of this picture would be necessary for the better understanding of the transition between cloud lines and waves.

A small cloud line is found to originate from a spot where no island is shown on the map. The spot might correspond to where sea-surface temperature is higher than the environment.

Presented in Fig. 12 is the upper-air temperature and dew-point temperature from Chatham Island. The lowest layer with the adiabatic lapse rate extends to 1.5 km where pressure is about 850 mb. It may be assumed that the plume clouds in SL 4-3705 are imbedded inside this adiabatic layer. The stable layer between the 1.5 and 3-km level is so dry that no clouds are in existence.

An attempt was made to rectify SL-3703 for detailed examination of the wake waves from Campbell Island (Fig. 13). There are two dominant peaks on the island, resulting in the two sources of wake waves.

A minor wake extends from the 465-m peak near the west end of the island. The major wake is originated by the highest peak of the island with a 569-m elevation.

A combined wake is rather complicated in places where two sets of waves intersect in acute angles. Unfortunately, no temperature sounding is available from Campbell Island within several hours from the picture time.

Winds aloft from Campbell shows the existence of a significant shear layer between 1.7 and 2.0-km level (Fig. 14). The advection line of the wake extending toward the 190° direction from the 569-m peak coincides with the flow direction of the lower layer below the shear layer. This would imply that the advection line is the trajectory of the air modified by the island. A similar trajectory of the surface water modified by

a ship is seen along the ship track.

The center line of the wake obtained by bisecting the V-shaped wake is oriented in the direction 340° to 170°. This orientation is very close to the mean value of the flow direction of the lower layer (010° -190°) and the upper layer (330° -150°). These figures indicate that the wake waves propagate with the mean velocity of the upper and lower layers.

8. DRY AND WET WAKES FROM ANTIPODES ISLAND

A significant change in the wake of Antipodes Island took place between December 16 and 17, 1973. Two Skylab pictures taken 23-hours apart revealed the change.

SL 4-3655 taken in Orbit 3110 on December 16, 1973 shows small patches of clouds on top of high peaks on Antipodes Island southeast of New Zealand. Although a distinct pattern of wake waves is visble in Fig. 15, these waves are not characterized by clouds. If cumuliform clouds are imbedded inside the waves, their brightness cannot be as low as they are on the picture.

Our suspicion is that the waves were made visible by the differential depth of pollutants trapped beneath the inversion layer. Namely, more pollutants are to be found beneath the crests while less pollutants will exist beneath the troughs. Such waves may be identified as "dry waves". On the other hand, wake waves with condensed water droplets or cloud may be called "wet waves". Figure 5 indicates the wave length of the transverse waves is about 10 km.

Figure 16 shows a picture of SL 4-3668 taken at 0020 GMT December 17, 23hr07min after the previous picture. Significant "wet waves" are seen behind the same island. A considerable change in the flow direction also took place.

Figure 17 was prepared to show the difference in the surface weather maps within 24 hours. A major change appears to be the advancement of a cyclone toward the east-northeast. The flow direction at the location of Antipodes Island shifted from westerly to northerly. Meanwhile, clouds of all types moved in.

The surface weather maps also indicate a good possibility that the pollution from New Zealand is likely to move in the area of Antipodes which is located downwind.

The stratification at the lowest layer just above the sea surface has been examined. As presented in Fig. 18, the lapse rate below the inversion top at the 2.5-km level was almost isothermal almost all-the-way to the sea level.

If we assume that the stratification at Campbell Island is applied to Antipodes Island, at least in characteristics, the lapse rate is favorable for the wave propagation. Such a stable lapse rate will minimize the kinetic energy dissipation through eddy transport of low-level momentum.

CONCLUSIONS

Examination of mesoscale cloud patterns within the wake of obstacles seen in Skylab pictures reveal the existence of specific types of wake clouds related to meteorological conditions. They are:

A. Cumulus streets occurring when the lapse rate above the surface is adiabatic with a medium to slow flow speed.

B. Kármán Vortex Streets occurring when the lapse rate above the surface is small, zero, or negative with a slow to medium speed flow impinging against a relatively large obstacle.

C. Wake waves occurring when the lapse rate above the surface is small with a medium to fast speed flow impinging against a relatively small obstacle. When the flow speed exceeds a critical value the transverse waves tend to disappear, leaving the diverging waves only.

It may be concluded that the human decision in taking pictures of specific phenomena as viewed from a space platform is of extreme value and importance. There are always large chances that new phenomena can be found and photographed efficiently.

Skylab photography has demonstrated the values of human judgment in picture taking which cannot be made otherwise.

It is expected that other features in Skylab pictures are investigated before or even after the termination of the current contract No. NAS 9-14042 with Johnson Space Center.

Future results are to be sent to JSC upon completion of additional studies.

REFERENCES

Briggs, G. A. and C. B. Leovy (1974): Mariner 9 Observations of the Mars North Polar Hood. Bulletin of the American Meteorological Society. Vol. 55, No. 4, pp. 278-296.

Chopra, K. P. and L. F. Hubert (1964): Kármán Vortex Streets in Earth's Atmosphere. Nature. Vol. 23, No. 4952, pp. 1341-1343.

_____ and _____(1965): Kármán Vortex Streets in Wakes of Islands. Journal of the American Institute of Aeronautics and Astronautics. Vol. 3, No. 10, pp. 1941-1943.

Havelock, T. H. (1950): Wave Resistance Theory and its Application to Ship Problems. Society of Naval Architects and Marine Engineers, New York.

Kelvin, Lord (1887): On the Waves Produced by a Single Impulse in Water of any Depth, or in a Dispersive Medium. Proceedings of the Royal Society of London. Ser. A, Vol. 42, pp. 80-85.

Stoker, J. J. (1957): Water Waves, The Mathematic Theory with Applications. Interscience Publishers, New York, 567 pp.

Tsuchiya, K. and T. Fujita (1966): A Satellite Meteorological Study of Evaporation and Cloud Formation over the Western Pacific under the Influence of the Winter Monsoon. SMRP Research Paper 55, The University of Chicago, 33 pp.

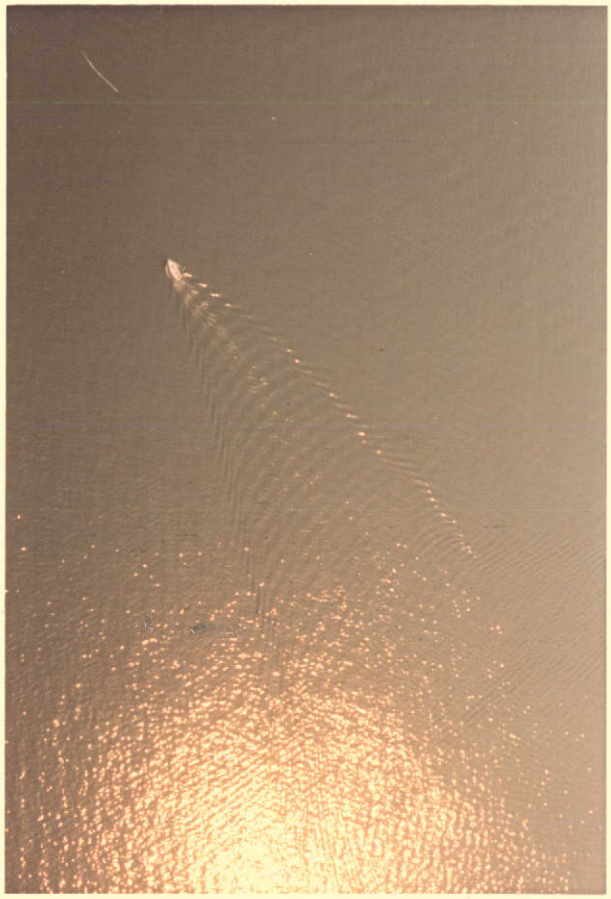

Fig. 2. Wake waves from a slow-moving boat.

Fig. 3. Wake waves behind a speed boat.

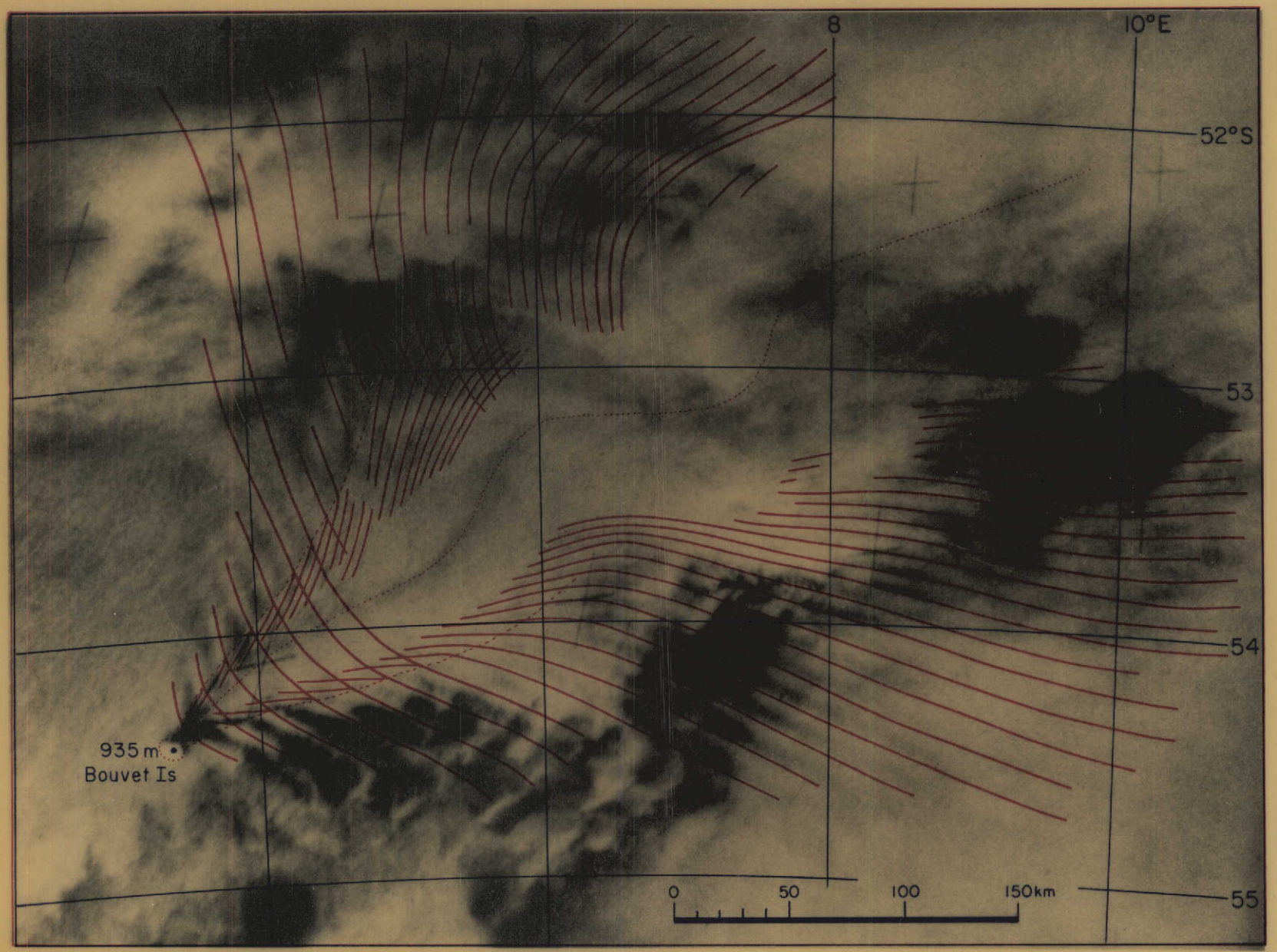

Fig. 1. Wake waves from Bouvet Island in the South Atlantic. Semi-rectified picture of SL-4-3633 taken 1423 GMT, December 15, 1973.

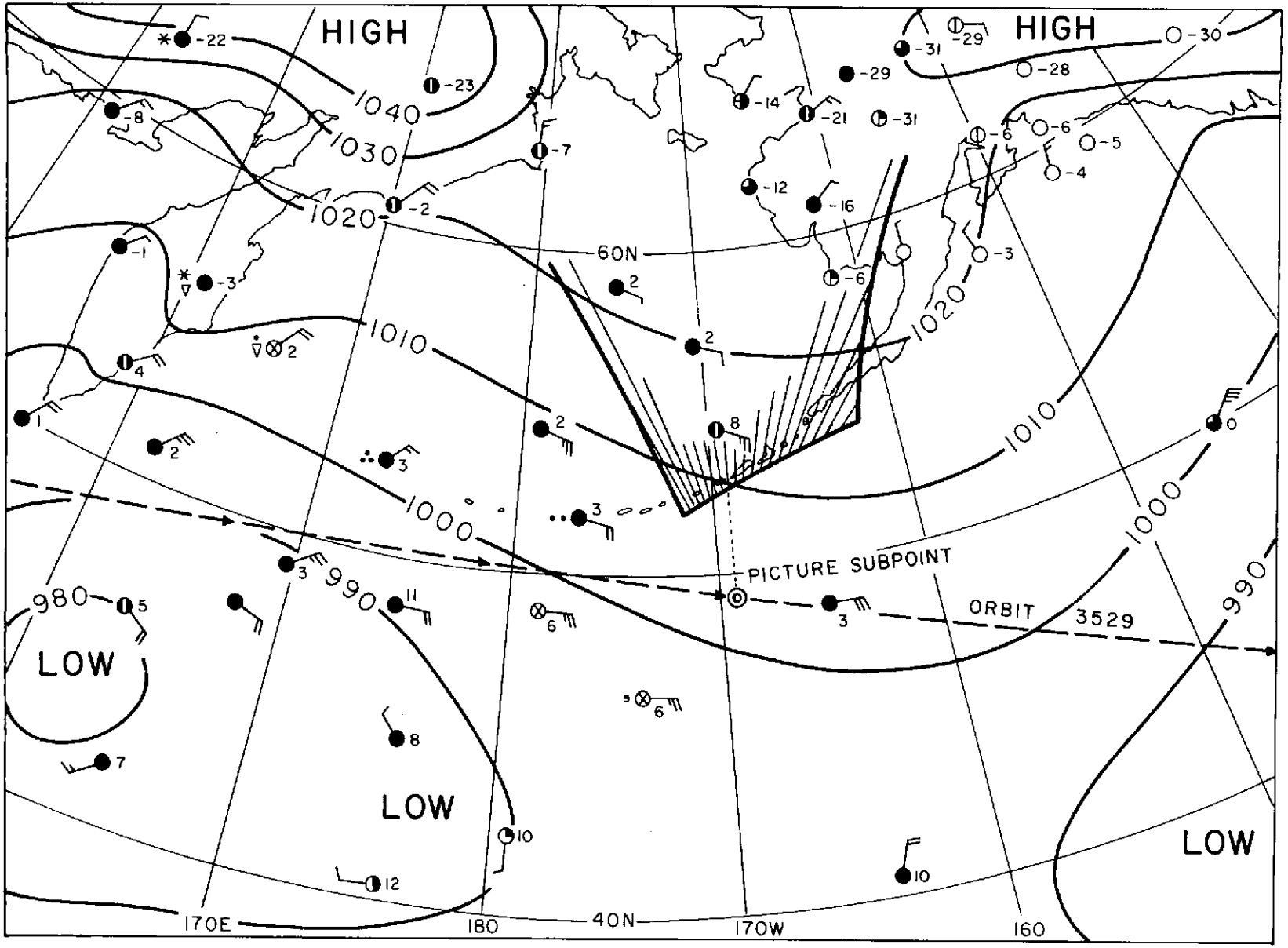

Fig. 4. The area of the cloud picture in Fig. 5 superimposed upon the surface chart at 0000 Z January 14, 1974.

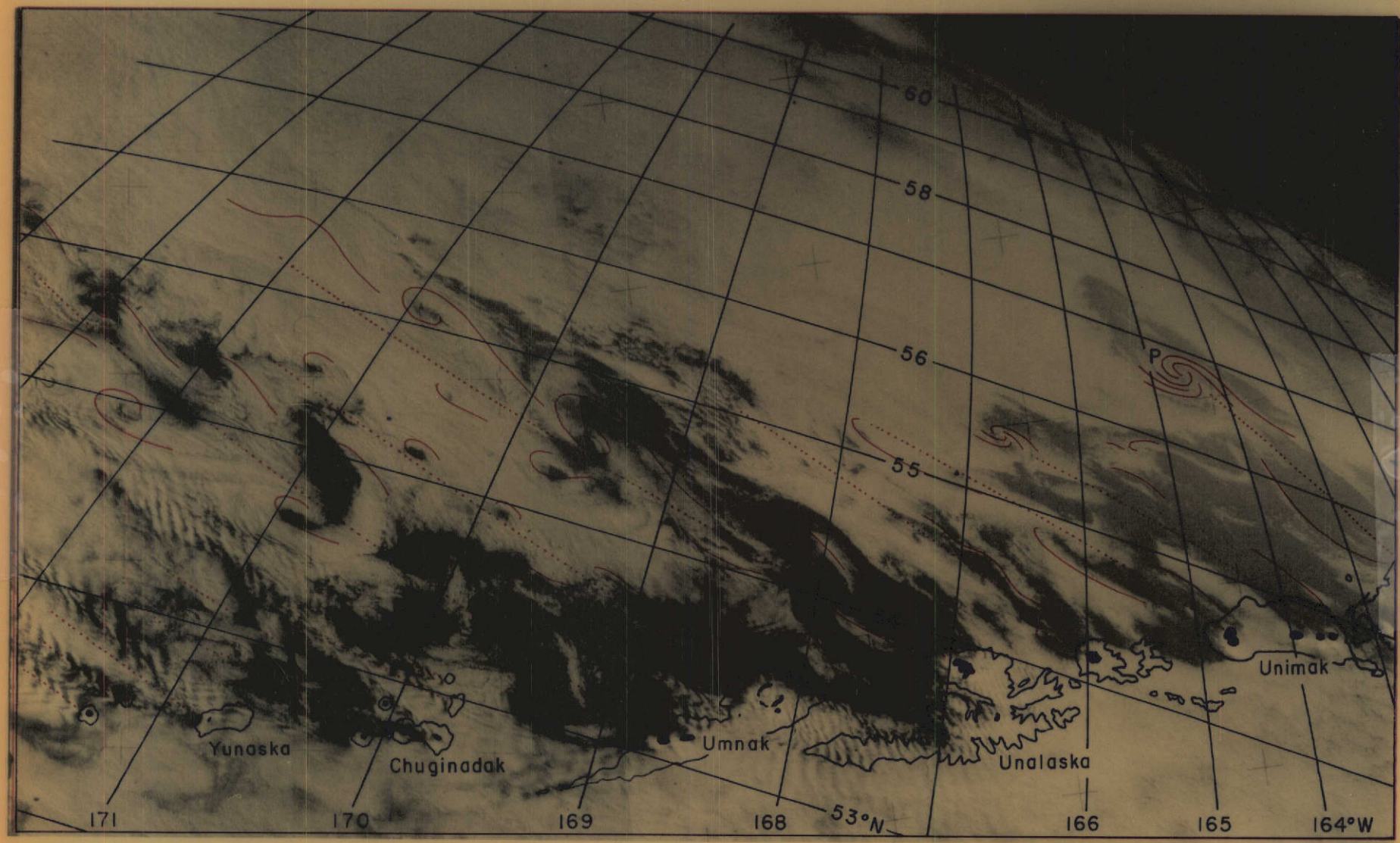

Fig. 5. Kármán vortex streets and island wakes from Aleutian Islands. A composite picture from SL 4-140-4111 and 4112 taken at 0143 Z January 14, 1974. Areas above 1000-m elevation are painted.

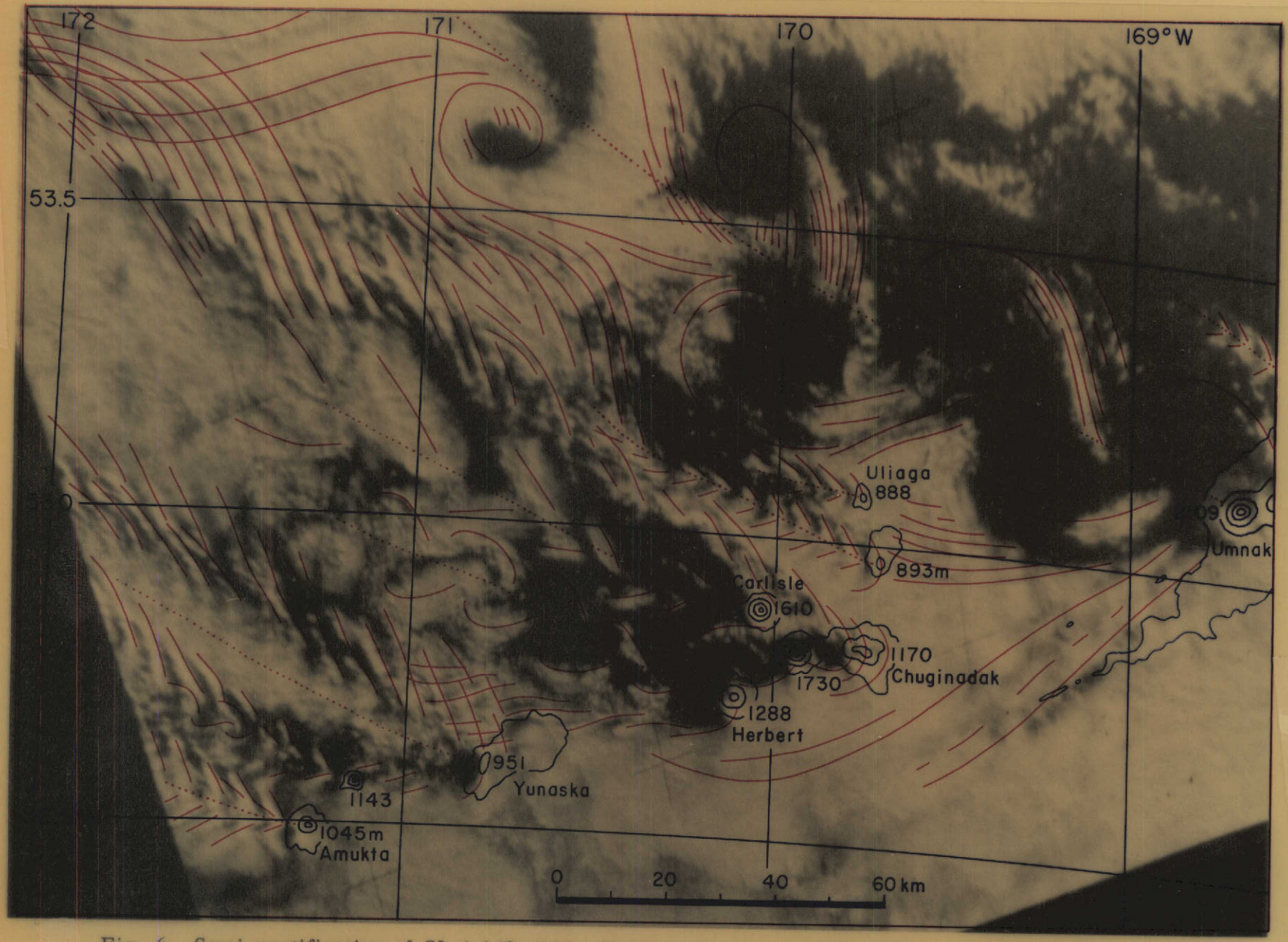

Fig. 6. Semi-rectification of SL 4-140-4111. Height contours are 500, 1000, and 1500 m MSL.

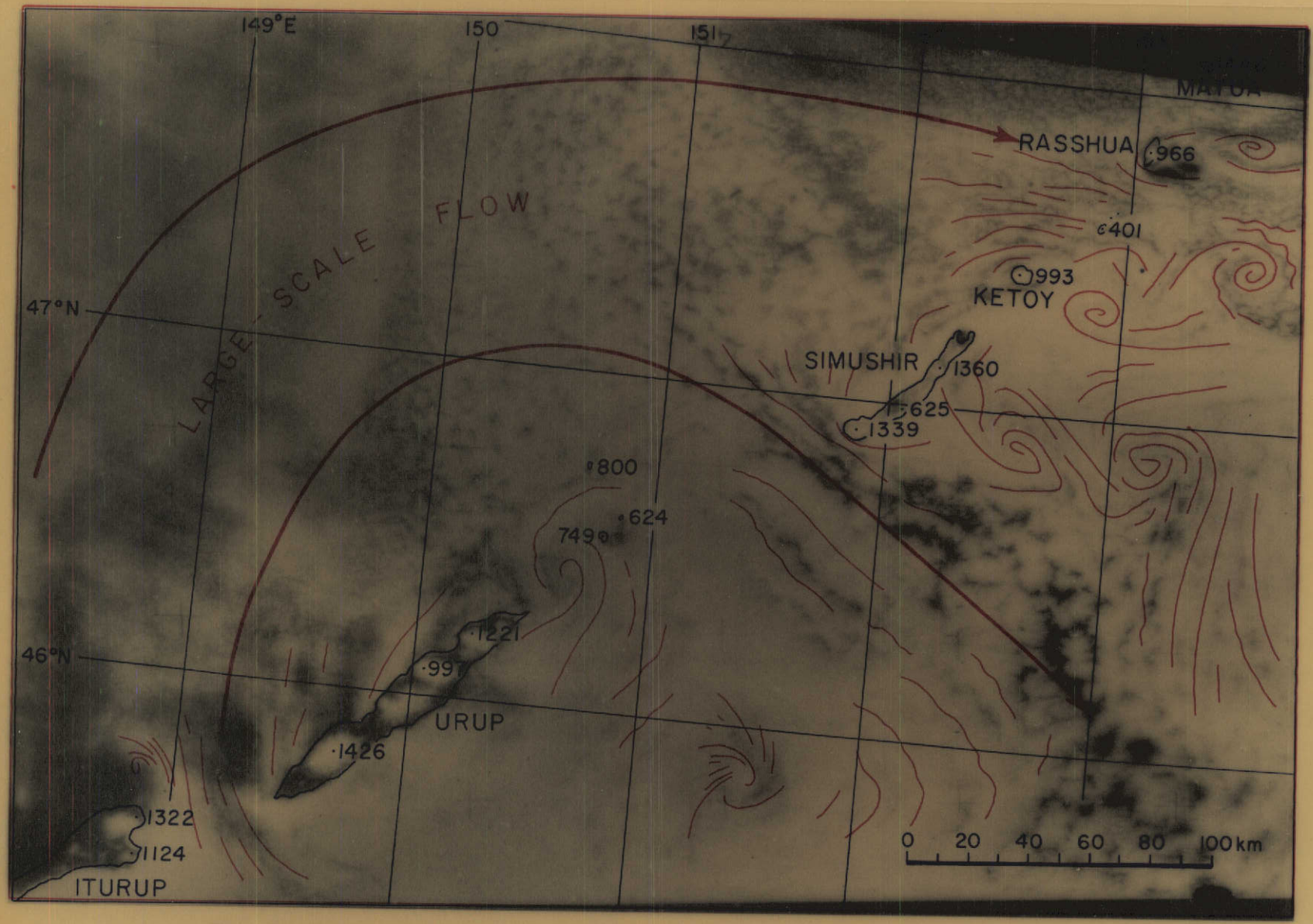

Fig. 7. Semi-rectified picture of SL 2-5-432 showing Karman vortex streets from Kuril islands.

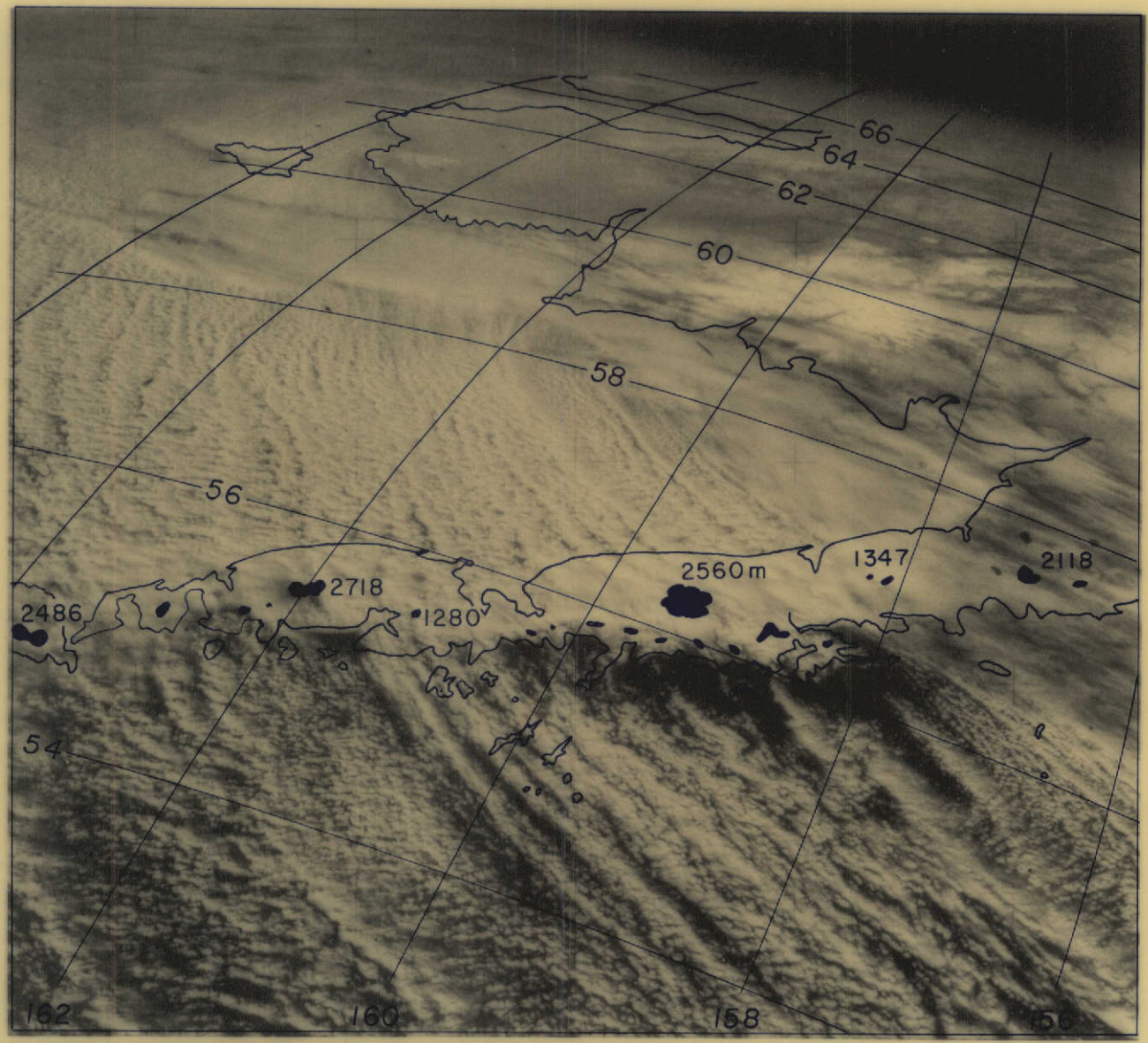

Fig. 8. Blocking of evaporation cumulus streets by Aleutian island. Grid lines and landmarks placed on SL 4-140-4210 taken at 0106 Z January 17, 1974.

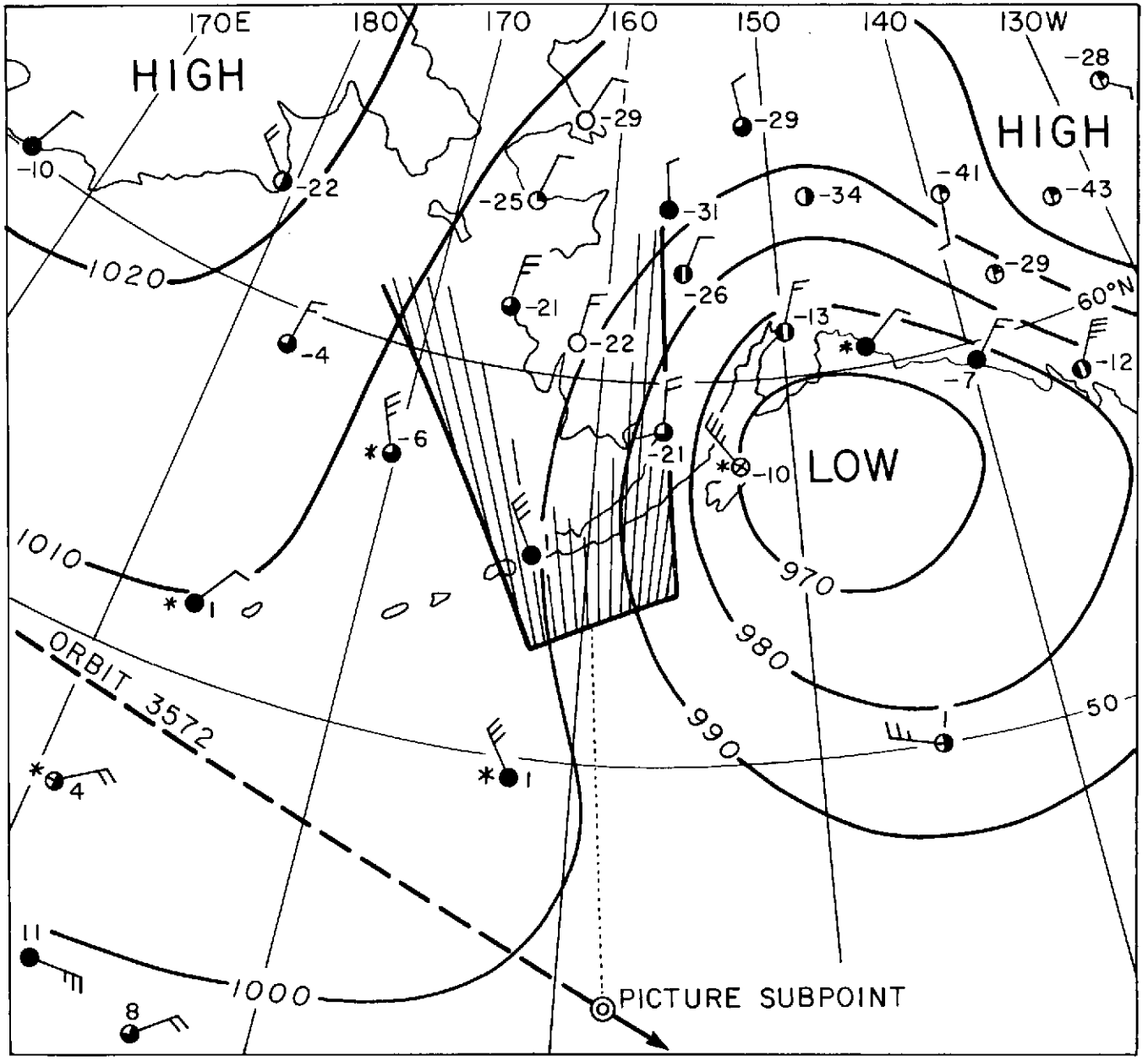

Fig. 9. Surface map for 0000 Z January 17, 1974 corresponding to the time of SL 4-140-4210.

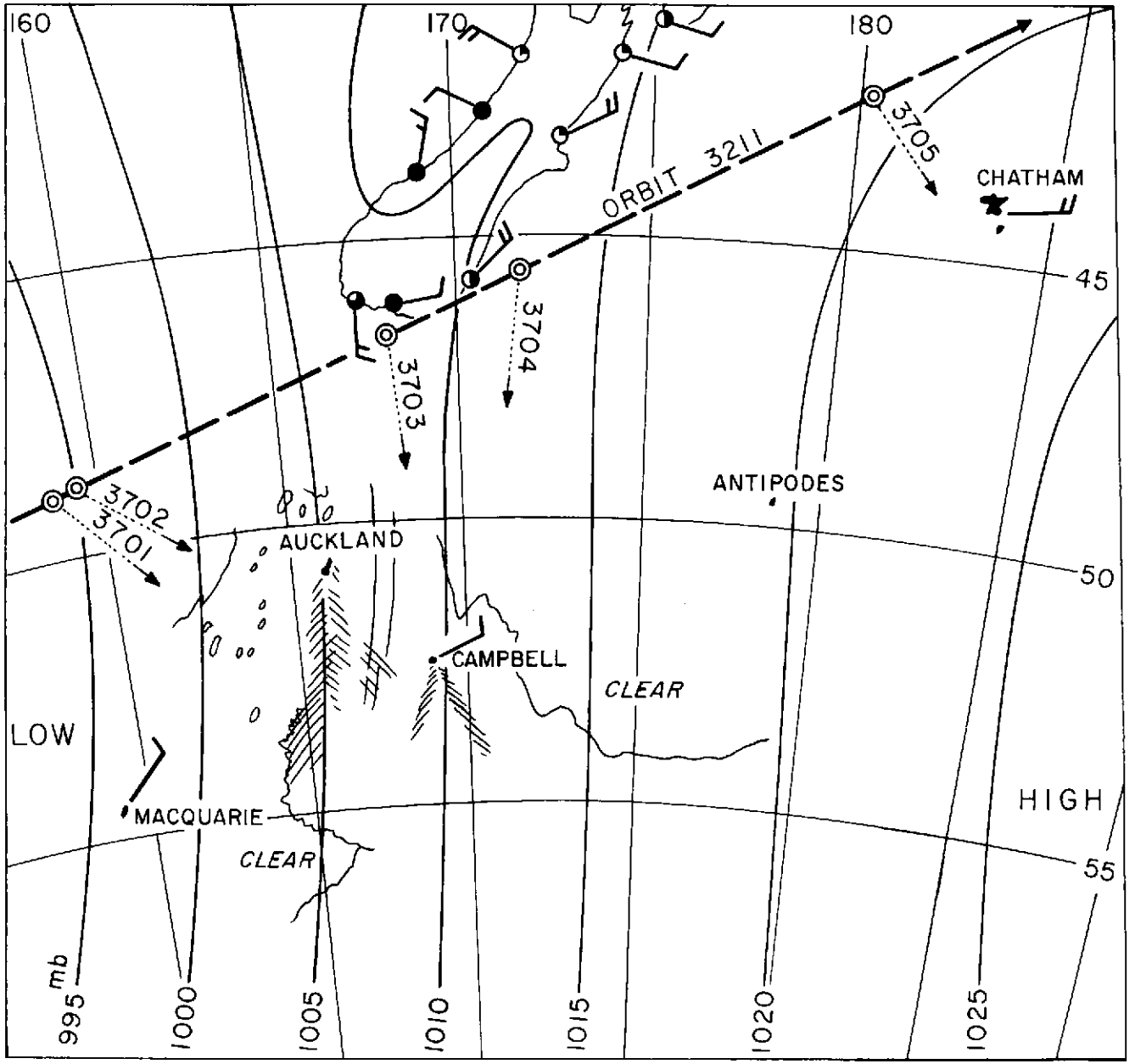

Fig. 10. Surface map for 0000 Z December 23, 1973. SL 4-137-3701 through 3705 were photographed at the locations of double circles.

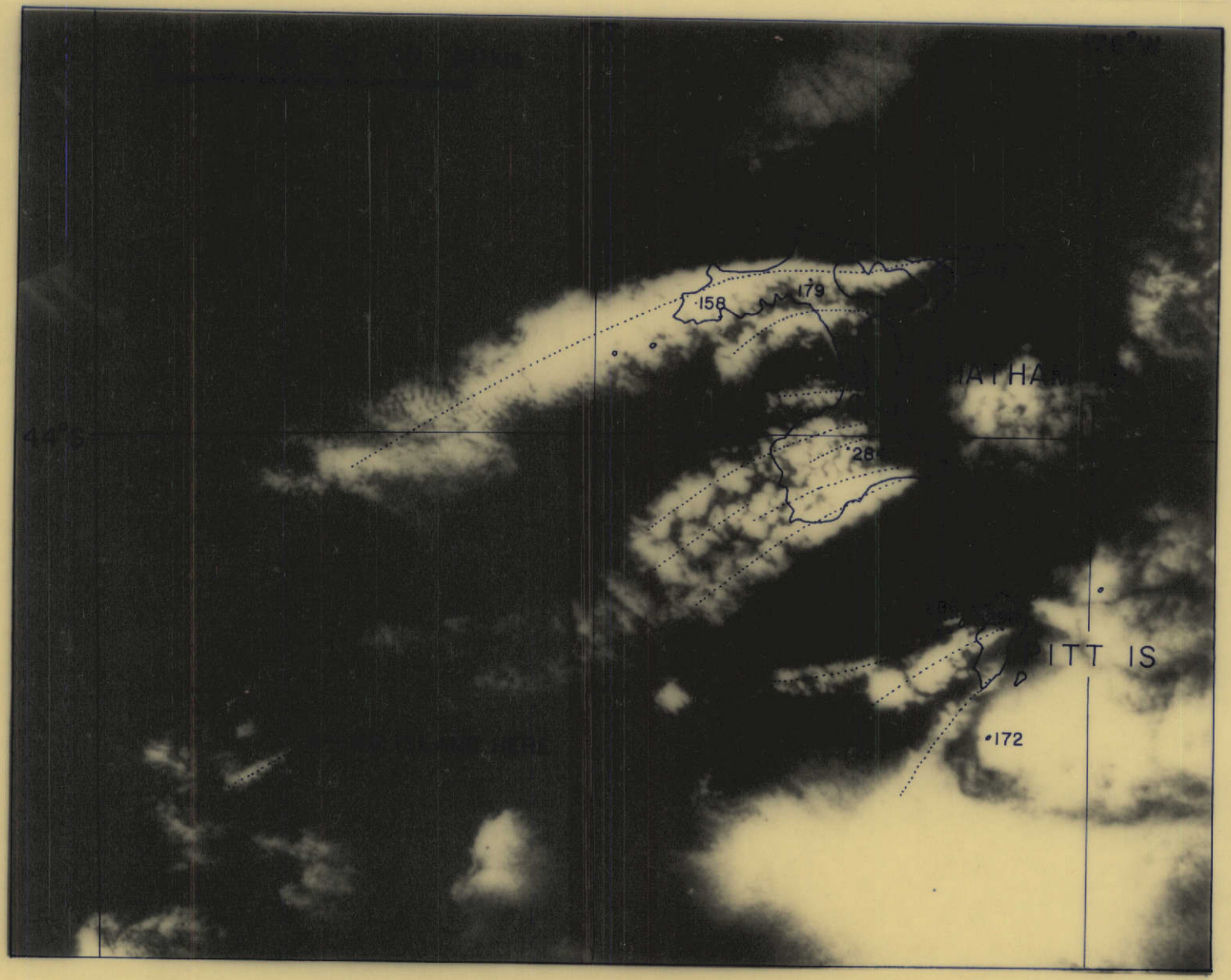

Fig. 11. Cumulus streets from Chatham island seen in a rectified picture of SL 4-137-3705, 0114 Z December 23, 1973.

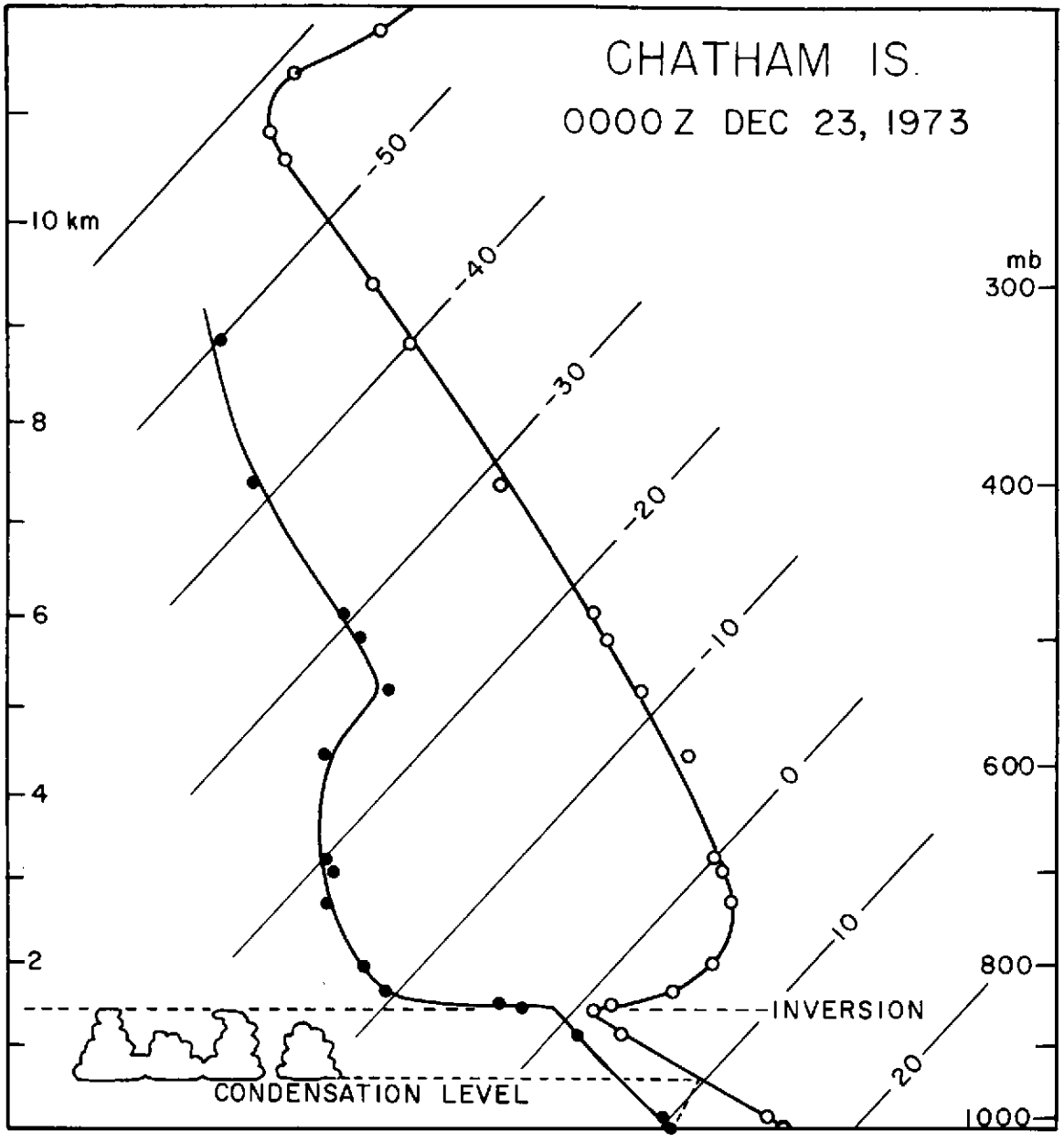

Fig. 12. Sounding at Chatham made 1 hr 14 min prior to the time of SL 4-137-3705.

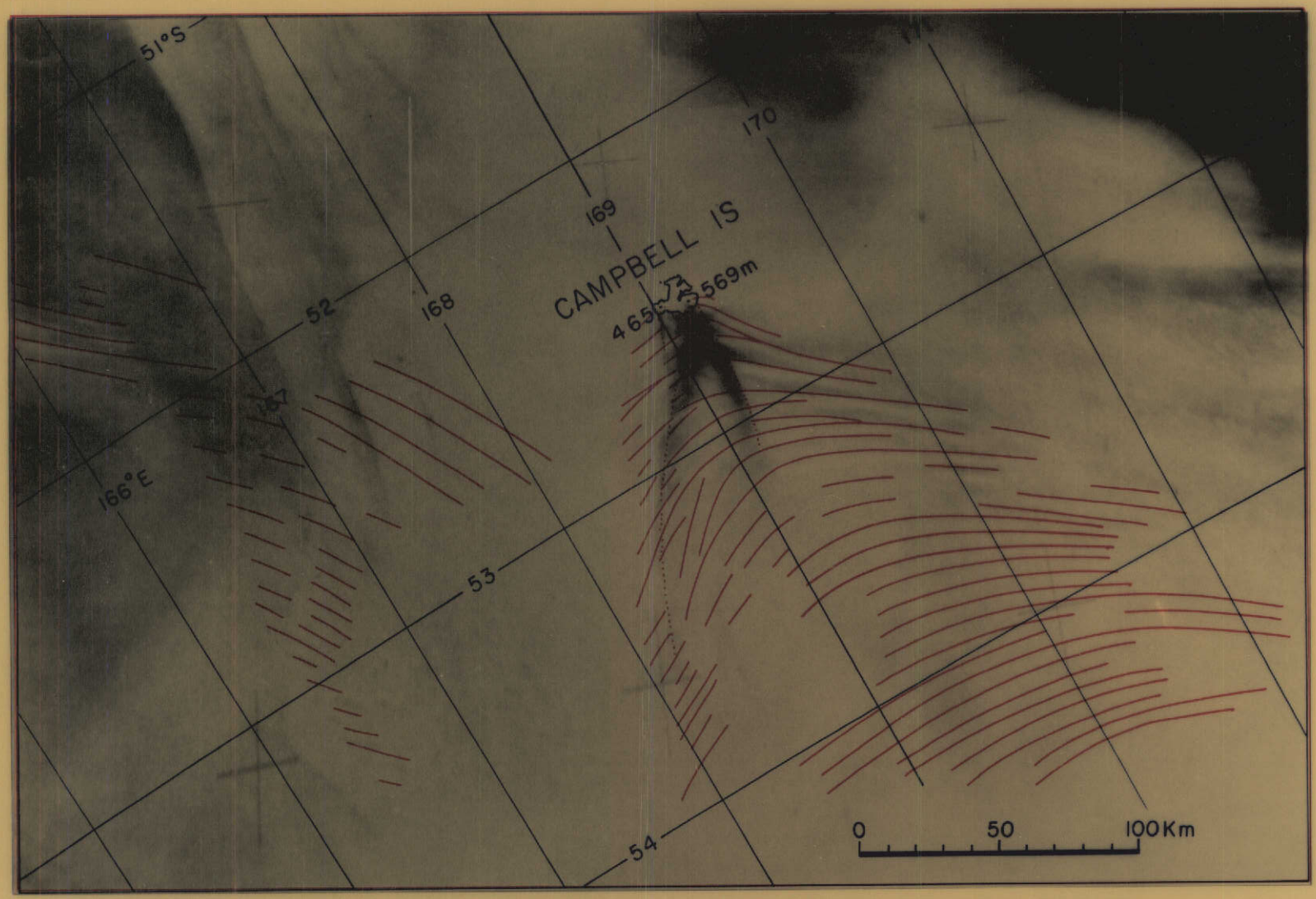

Fig. 13. Wake waves from Campbell and Auckland Islands south of New Zealand. Enlargement of SL 4-3703. 0111 Z December 23, 1973.

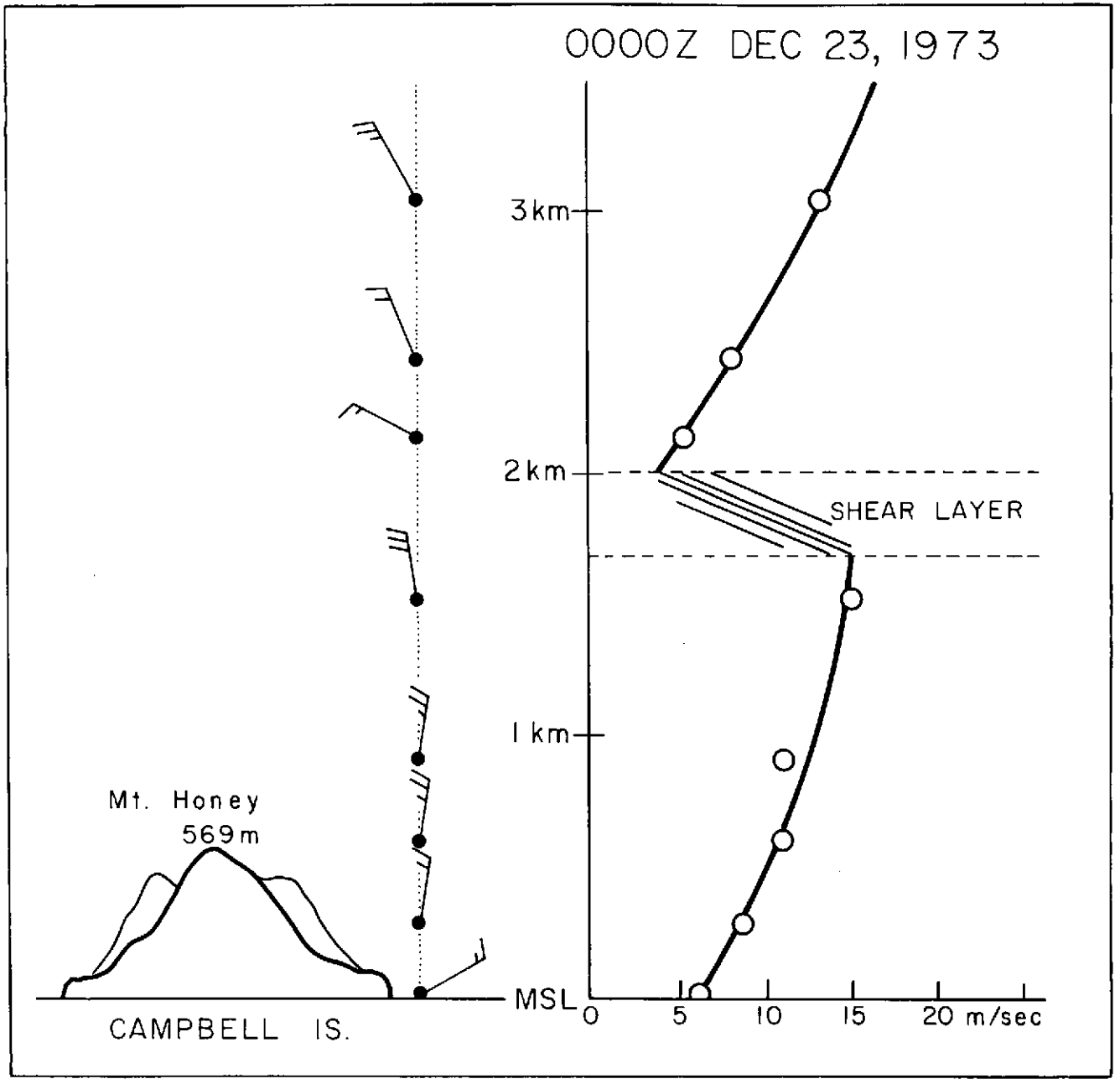

Fig. 14. Vertical distribution of winds over Campbell Island at 0000 Z December 23, 1973.

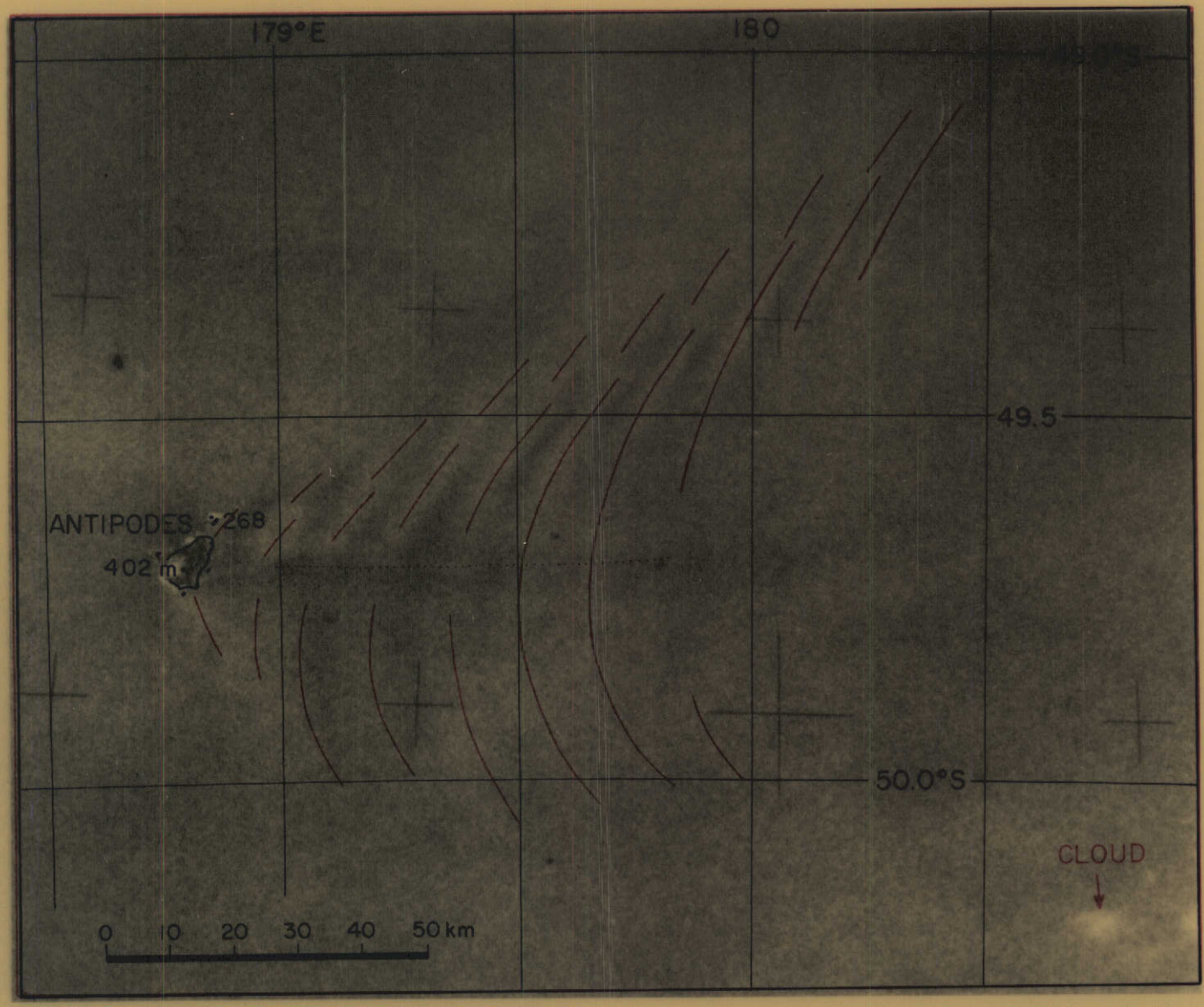

Fig. 15. Wake waves behind Antipodes Island made visible by the differential thickness of air pollutants. Dry wakes without clouds. Rectification of SL 4-137-3655 taken at 0113 Z December 16, 1973.

Fig. 16. Wake waves behind Antipodes Island made visible by wave clouds. Wet wakes with clouds. SL 4-137-3668 taken at 0020 Z December 17, 1973.

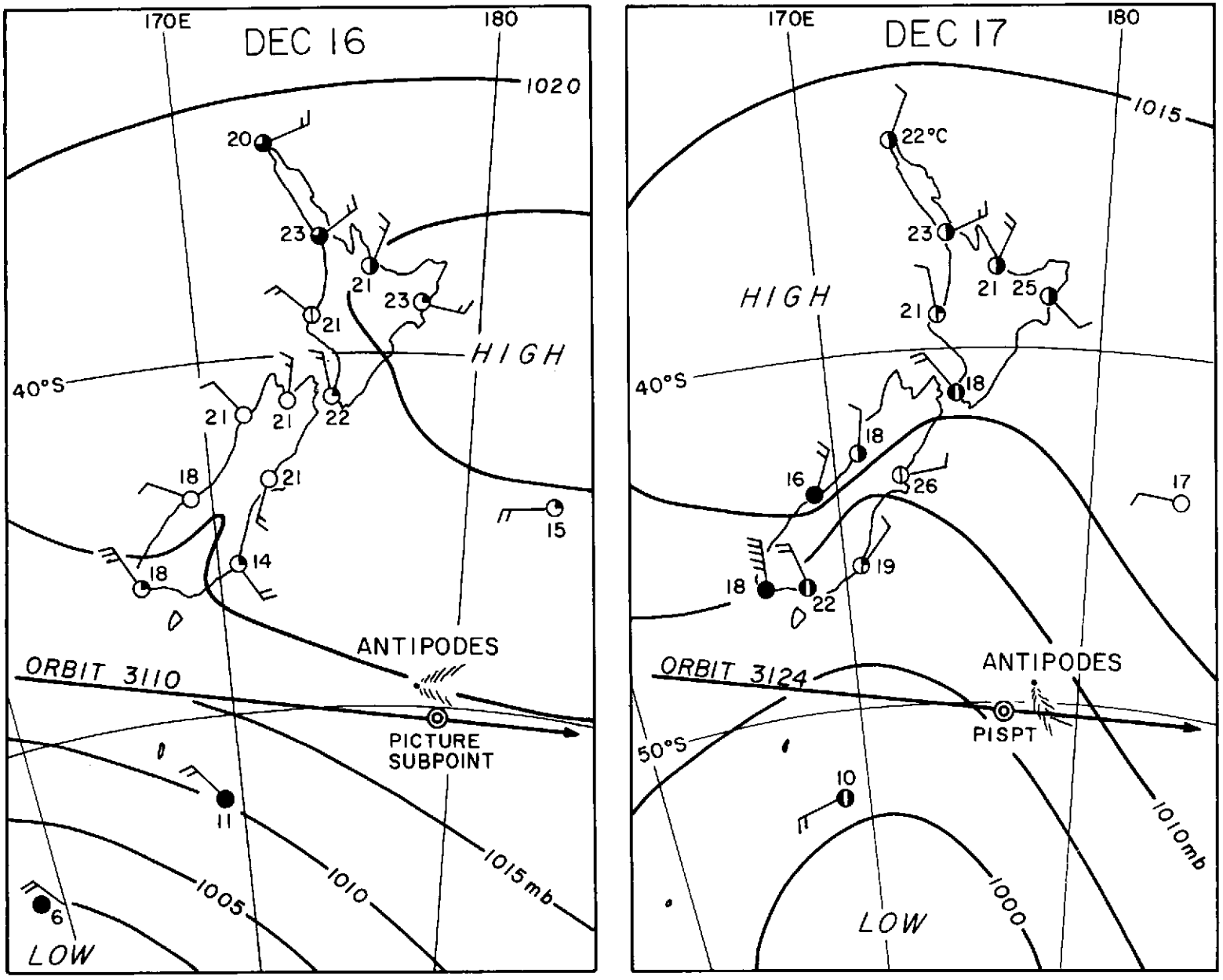

Fig. 17. Change in the surface flow during the 24-hr period, 0000 Z December 16-17, 1973.

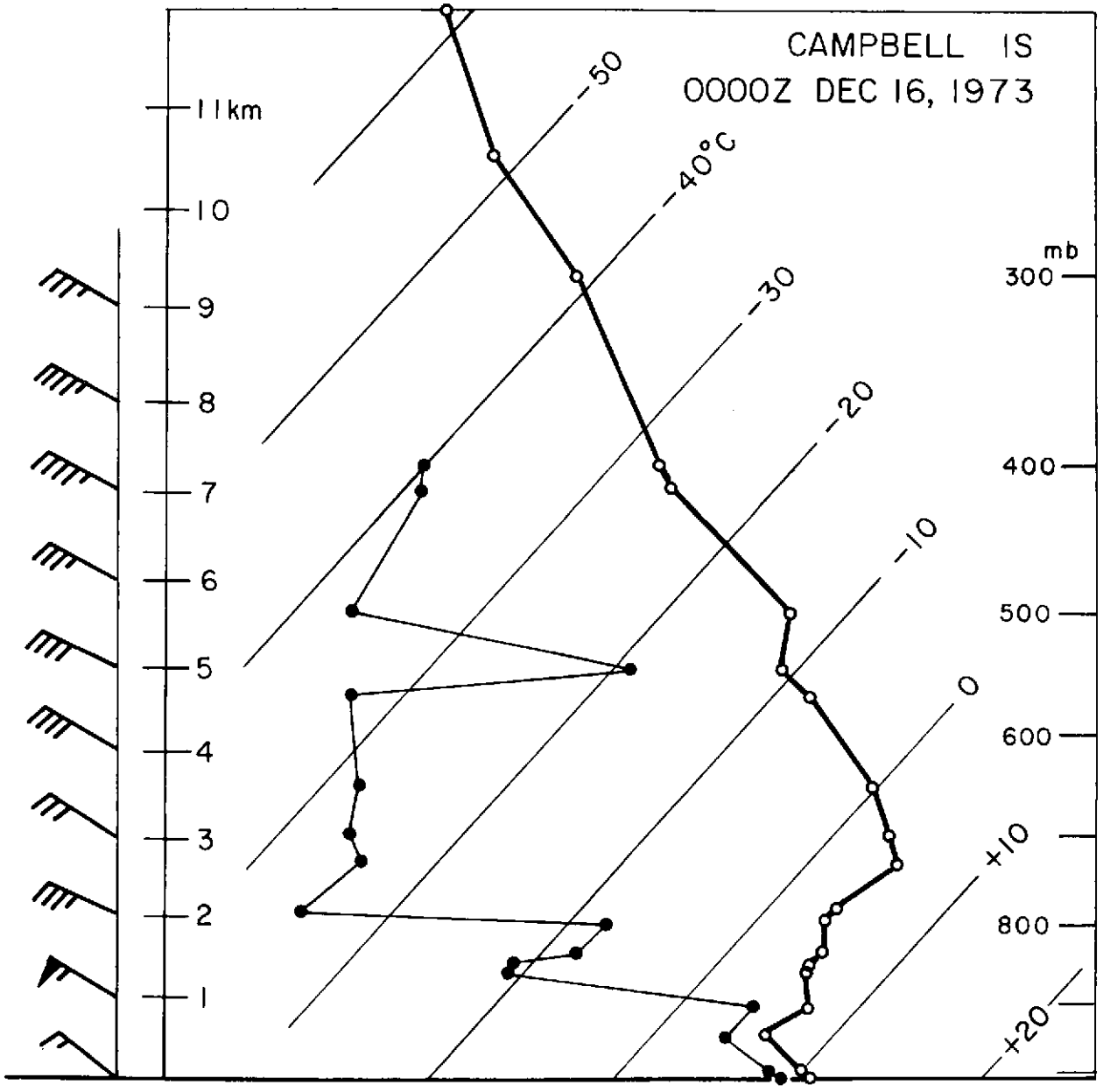

Fig. 18. Vertical distribution of temperature and wind from Campbell Island at 0000 Z December 16, 1973.